0022-3565/09/3312-591–597$20.00
THE JOURNAL OF PHARMACOLOGY AND EXPERIMENTAL THERAPEUTICS
JPET 331:591–597, 2009

Vol. 331, No. 2
158162/3523384
Printed in U.S.A.

Blockade of 2-Arachidonoylglycerol Hydrolysis by Selective Monoacylglycerol Lipase Inhibitor 4-Nitrophenyl 4-(Dibenzo[*d*][1,3]dioxol-5-yl(hydroxy)methyl)piperidine-1-carboxylate (JZL184) Enhances Retrograde Endocannabinoid Signaling

Bin Pan, Wei Wang, Jonathan Z. Long, Dalong Sun, Cecilia J. Hillard, Benjamin F. Cravatt, and Qing-song Liu

Department of Pharmacology and Toxicology, Medical College of Wisconsin, Milwaukee, Wisconsin (B.P., W.W., D.S., C.J.H., Q.-S.L.); The Skaggs Institute for Chemical Biology, Department of Chemical Physiology, The Scripps Research Institute, La Jolla, California (J.Z.L., B.F.C.)

Received June 26, 2009; accepted August 7, 2009

ABSTRACT

Endocannabinoid (eCB) signaling mediates depolarization-induced suppression of excitation (DSE) and inhibition (DSI), two prominent forms of retrograde synaptic depression. *N*-Arachidonoylethanolamine (AEA) and 2-arachidonoylglycerol (2-AG), two known eCBs, are degraded by fatty acid amide hydrolase (FAAH) and monoacylglycerol lipase (MAGL), respectively. Selective blockade of FAAH and MAGL is critical for determining the roles of the eCBs in DSE/DSI and understanding how their action is regulated. 4-Nitrophenyl 4-(dibenzo[*d*][1,3]dioxol-5-yl(hydroxy)methyl)piperidine-1-carboxylate (JZL184) is a recently developed, highly selective, and potent MAGL inhibitor that increases 2-AG but not AEA concentrations in mouse brain. Here, we report that JZL184 prolongs DSE in Purkinje neurons in cerebellar slices and DSI in CA1 pyramidal neurons in hippocampal slices. The effect of JZL184 on DSE/DSI is mimicked by the nonselective MAGL inhibitor methyl arachidonyl fluorophosphonate. In contrast, neither the selective FAAH inhibitor cyclohexylcarbamic acid 3′-carbomoylbiphenyl-3-yl ester (URB597) nor FAAH knockout has a significant effect on DSE/DSI. JZL184 produces greater enhancement of DSE/DSI in mouse neurons than that in rat neurons. The latter finding is consistent with biochemical studies showing that JZL184 is more potent in inhibiting mouse MAGL than rat MAGL. These results indicate that the degradation of 2-AG by MAGL is the rate-limiting step that determines the time course of DSE/DSI and that JZL184 is a useful tool for the study of 2-AG-mediated signaling.

Depolarization-induced suppression of excitation (DSE) and inhibition (DSI) are arguably the best-characterized forms of retrograde synaptic transmission in the brain. DSE and DSI are mediated by endocannabinoid (eCB) signaling since they were blocked by type I cannabinoid (CB1) receptor antagonists (Kreitzer and Regehr, 2001; Ohno-Shosaku et al., 2001; Wilson and Nicoll, 2001). The eCB system has at least two endogenous ligands, *N*-arachidonoylethanolamine (AEA) and 2-arachidonoylglycerol (2-AG), that activate the CB1 receptor (Di Marzo et al., 1998). AEA and 2-AG are produced and released "on demand" in response to depolarization-induced calcium influx (Stella et al., 1997; Di Marzo et al., 1998) and/or the activation of certain G-protein-coupled receptors, such as group I metabotropic glutamate receptors (Maejima et al., 2001; Jung et al., 2005). The biosynthetic processes probably regulate the onset of eCB-mediated

This work was supported by National Institutes of Health [Grants DA09155, DA017259, DA024741] (to C.J.H., B.F.C., and Q.S.L., respectively); the National Alliance for Research on Schizophrenia and Depression (to Q.S.L.); and the Advancing in a Healthier Wisconsin (to C.J.H. and Q.S.L.).
Article, publication date, and citation information can be found at http://jpet.aspetjournals.org.
doi:10.1124/jpet.109.158162.

ABBREVIATIONS: DSE, depolarization-induced suppression of excitation; DSI, depolarization-induced suppression of inhibition; ABPP, activity-based protein profiling; 2-AG, 2-arachidonoylglycerol; ACSF, artificial cerebrospinal fluid; AEA, *N*-arachidonoylethanolamine; AM251, 1-(2,4-dichlorophenyl)-5-(4-iodophenyl)-4-methyl-*N*-(1-piperidyl)pyrazole-3-carboxamide; CNQX, 6-cyano-7-nitroquinoxaline-2,3-dione; COX-2, cyclooxygenase-2; D-AP-5, D-2-amino-5-phosphonovaleric acid; DMSO, dimethyl sulfoxide; eCB, endocannabinoid; EPSCs, excitatory postsynaptic currents; FAAH, fatty acid amide hydrolase; IPSCs, inhibitory postsynaptic currents; JZL184, 4-nitrophenyl 4-(dibenzo[*d*][1,3]dioxol-5-yl(hydroxy)methyl)piperidine-1-carboxylate; MAFP, methyl arachidonyl fluorophosphonate; MAGL, monoacylglycerol lipase; QX-314, *N*-(2,6-dimethylphenylcarbamoylmethyl)triethylammonium bromide; URB597, cyclohexylcarbamic acid 3′-carbomoylbiphenyl-3-yl ester; URB602, biphenyl-3-ylcarbamic acid cyclohexyl ester; URB754, 6-methyl-2-[(4-methylphenyl)amino]-4*H*-3,1-benzoxazin-4-one.

signaling. However, the duration of eCB-mediated signaling and a possible basal tone are probably regulated by their catabolic inactivation. The primary enzymes for the catabolism of AEA and 2-AG are fatty acid amide hydrolase (FAAH) and monoacylglycerol lipase (MAGL), respectively (Cravatt et al., 1996; Blankman et al., 2007). Selective blockade of FAAH and MAGL is critical for determining the roles of the eCBs in DSE/DSI and understanding how the time course of DSE/DSI is regulated.

Previous studies have shown that the FAAH inhibitor URB597 does not affect DSE/DSI, whereas agents that inhibit both AEA and 2-AG degradative pathways, including cyclooxygenase-2 (COX-2) inhibitors and nonselective serine hydrolase inhibitors [e.g., methyl arachidonyl fluorophosphonate (MAFP), URB602] prolong DSE/DSI (Kim and Alger, 2004; Makara et al., 2005; Straiker and Mackie, 2005; Szabo et al., 2006; Hashimotodani et al., 2007). However, these inhibitors have multiple bioactive targets and, in particular, do not discriminate between 2-AG and AEA degradative pathways (Lio et al., 1996; De Petrocellis et al., 1997; Kozak et al., 2000). For instance, URB602, the best characterized MAGL inhibitor, displays an IC_{50} value of ~200 μM against MAGL activity (King et al., 2007) and inhibits FAAH with similar potency (Vandevoorde et al., 2007). MAFP, another MAGL inhibitor, inhibits phospholipases (Lio et al., 1996), FAAH (De Petrocellis et al., 1997), and other serine hydrolases that use lipid substrates (Simon and Cravatt, 2008).

Selective MAGL inhibitors, including *N*-arachidonoylmaleimide (Saario et al., 2005), OMDM169 (Bisogno et al., 2009), and JZL184 (Long et al., 2009a), have become available in recent years. Among them, JZL184 is perhaps the most potent and selective MAGL inhibitor. JZL184 shows very high selectivity in inhibiting MAGL over FAAH and displays IC_{50} values of 6 to 8 nM and 4 μM for inhibition of mouse brain membrane MAGL and FAAH, respectively. Systemic administration of JZL184 to mice produced an eightfold increase in brain 2-AG levels without altering AEA and induced a broad array of CB1 receptor-dependent behavioral effects, including analgesia, hypothermia, and hypomotility (Long et al., 2009a). Although MAGL is capable of hydrolyzing monoacylglycerols other than 2-AG (Ho and Hillard, 2005), JZL184 has only minimal effect on other monoacylglycerols (Long et al., 2009a).

In the present study, we examined the effects of JZL184 on both DSE and DSI. We show that JZL184 produces robust potentiation of DSE in cerebellar Purkinje neurons and DSI in hippocampal CA1 pyramidal neurons, whereas neither genetic deletion of FAAH nor the selective FAAH inhibitor URB597 affects DSE/DSI. These data provide further evidence that 2-AG is the eCB mediator of DSE/DSI and that the degradation of 2-AG by MAGL determines the duration of eCB-mediated retrograde synaptic depression.

Materials and Methods

Slice Preparation. All animal use was in accordance with protocols approved by the Institution's Animal Care and Use Committee of Medical College of Wisconsin. C57BL/6J mice, FAAH knockout, and wild-type mice and Sprague-Dawley rats were anesthetized by isoflurane inhalation and decapitated. Genotype was confirmed by polymerase chain reaction with use of a DNA sample obtained from the ear. Cerebellar or hippocampal slices were cut by use of a vibrating slicer (Leica Microsystems, Deerfield, IL). Sagittal slices (250 μm thick) were cut from the cerebellar vermis of 10- to 14-day-old animals, and transverse slices (300 μm thick) were cut from the hippocampus of 15- to 21-day-old animals. Slices were prepared at 4 to 6°C in a solution containing 220 mM sucrose, 2.5 mM KCl, 1.25 mM NaH_2PO_4, 0.5 mM $CaCl_2$, 7 mM $MgSO_4$, 26 mM $NaHCO_3$, 10 mM glucose, and 1 mM sodium ascorbate. The slices were incubated at 32 to 34°C for 30 to 40 min in the following solution: 110 mM sucrose, 65 mM NaCl, 2.5 mM KCl, 2.5 mM $CaCl_2$, 1 mM $MgCl_2$, 1.25 mM NaH_2PO_4, 26 mM $NaHCO_3$, 10 mM glucose, and 1 mM sodium ascorbate. The slices were transferred to and stored in artificial cerebrospinal fluid (ACSF) containing 119 mM NaCl, 2.5 mM KCl, 2.5 mM $CaCl_2$, 1 mM $MgCl_2$, 1.25 mM NaH_2PO_4, 26 mM $NaHCO_3$, and 10 mM glucose at room temperature until use. All solutions were saturated with 95% O_2 and 5% CO_2.

Electrophysiology. Whole-cell recordings were made by use of a patch clamp amplifier (MultiClamp 700B; Molecular Devices, Sunnyvale, CA) under infrared-differential interference contrast microscopy. Data acquisition and analysis were performed using a digitizer (DigiData 1440A) and analysis software pClamp 10 (Molecular Devices). Signals were filtered at 2 kHz and sampled at 10 kHz. Excitatory postsynaptic currents (EPSCs) were recorded from cerebellar Purkinje neurons, and parallel fibers were stimulated with a bipolar tungsten electrode placed in the molecular layer. $GABA_A$ receptor blocker picrotoxin (50 μM) was present in the ACSF throughout the experiments. Glass pipettes (3–5 MΩ) were filled with an internal solution containing 130 mM cesium methanesulfonate, 10 mM CsCl, 5 mM QX-314, 10 mM HEPES, 0.2 mM EGTA, 2 mM $MgCl_2$, 4 mM MgATP, 0.3 mM Na_2GTP, and 10 mM Na_2-phosphocreatine (pH 7.2 with CsOH). To induce DSE, the cerebellar Purkinje neurons were depolarized from −60 mV to 0 mV for 1 s or 5 s, and EPSCs were evoked at 4-s intervals. To examine the effects of 2-AG and AEA on EPSCs, EPSCs were evoked at 10-s intervals.

Inhibitory postsynaptic currents (IPSCs) were recorded from hippocampal pyramidal neurons. A bipolar tungsten stimulation electrode was placed in the stratum radiatum of CA1 region of hippocampal slices to evoke IPSCs. Glutamate receptor antagonists 6-cyano-7-nitroquinoxaline-2,3-dione (CNQX, 20 μM) and D-2-amino-5-phosphonovaleric acid (D-AP-5, 50 μM) were present in the ACSF. The pipettes were filled with an internal solution containing 80 mM Cs-methanesulfonate, 60 mM CsCl, 5 mM QX-314, 10 mM HEPES, 0.2 mM EGTA, 2 mM $MgCl_2$, 4 mM MgATP, 0.3 mM Na_2GTP, and 10 mM Na_2-phosphocreatine (pH 7.2 with CsOH). To induce DSI, the CA1 pyramidal neurons were depolarized from −60 to 0 mV for 5 s, and IPSCs were evoked at 4-s intervals. Series resistance (15–30 MΩ) was monitored throughout the recordings, and data were discarded if the resistance changed by more than 20%. All recordings were performed at 32 ± 1°C by use of an automatic temperature controller.

All drugs were prepared as concentrated stock solutions and stored at −20 or −80°C before use. CNQX-Na (Sigma-Aldrich, St. Louis, MO) and D-AP-5 (Tocris Bioscience, Ellisville, MO) were dissolved in water. Picrotoxin (Sigma-Aldrich) was dissolved in ACSF through sonication. AM 251 (Tocris Bioscience), JZL184 (synthesized as described in Long et al., 2009a), URB597 (Biomol Research Laboratories, Plymouth Meeting, PA), and MAFP (Biomol) were dissolved in DMSO. AEA (Tocris Bioscience) and 2-AG (Tocris Bioscience) were dissolved in ethanol. When these drugs were used, control slices were treated in the same concentration of the respective solvent for similar exposure time. Drug-treated slices were interleaved with control slices from the same animal.

Data Analysis and Statistics. Data are presented as the mean ± S.E.M. EPSC and IPSC amplitudes were normalized to the baseline. The decay time constant (τ) of DSE and DSI was measured using a single exponential function of $y = y_0 + k \times \exp(-x/\tau)$. The magnitude of DSE/DSI was calculated as follows: DSE/DSI (%) = 100 × [1 − (mean of 3 EPSCs/IPSCs after depolarization/mean of 5 EPSCs/IPSCs before depolarization)]. Values of two to three DSE/DSI trials were averaged for each neuron. However, a single DSE

trial was performed on each neuron in Fig. 1C. The depression (percentage) of EPSCs by 2-AG or AEA was calculated as follows: 100 × [mean amplitude of 24 EPSCs after 2-AG or AEA treatment/mean amplitude of baseline EPSCs]. Data sets were compared with the Student's t test. Results were considered to be significant at $p < 0.05$.

Results

Effects of MAGL Inhibitor JZL184 on DSE and DSI. We investigated the effect of JZL184 on DSE in cerebellar Purkinje neurons and DSI in hippocampal CA1 pyramidal neurons, because DSE and DSI in these neuronal types are among the best characterized (Pitler and Alger, 1992; Kreitzer and Regehr, 2001; Ohno-Shosaku et al., 2001; Wilson and Nicoll, 2001). We first examined the effect of JZL184 on DSE in cerebellar Purkinje neurons. Whole-cell voltage-clamp recordings were made from Purkinje neurons in mouse cerebellar slices and EPSCs were evoked at 4-s intervals (see *Materials and Methods*). A brief depolarization (1 s from −60 to 0 mV) of Purkinje neurons induced a transient depression of EPSCs, or DSE, in every Purkinje neuron tested (Fig. 1A). Bath application of JZL184 for 40 to 120 min prolonged DSE in a dose-dependent manner, as shown by an increase in the mean decay time constant (τ) of DSE (Fig. 1, A and B). The half-maximal potentiation of τ was produced at 36.1 ± 6.2 nM (Fig. 1B). JZL184 had no significant effect on the magnitude of DSE (control, 49.5 ± 4.1%, $n = 8$; 100 nM JZL184, 63.6 ± 7.7%, $n = 6$; $p > 0.05$; for quantification of the magnitude of DSE/DSI, see *Materials and Methods*). Activity-based protein profiling (ABPP) of mouse brain membrane proteome has shown that JZL184 displays time-dependent inhibition of MAGL, and it takes ~40 min for JZL184 to produce the maximal inhibition of MAGL. A covalent mechanism of inactivation may underlie the time-dependent inhibition (Long et al., 2009a). Consistent with this study, we have found that full potentiation of DSE by JZL184 was seen after 40 min of incubation with JZL184. It is known that DSE is mediated by CB1 receptors (Kreitzer and Regehr, 2001). Indeed, we found that DSE induced in the presence or absence of JZL184 was abolished by preincubation and continuous application of CB1 receptor antagonist AM 251 (2 μM, $n = 3$ each, data not shown). The potentiation of DSE by JZL184 (1 μM) was even more pronounced when longer depolarization (5 s) was used to induce DSE (τ: control, 20.7 ± 4.6 s, $n = 8$; JZL184, 200.5 ± 36.7 s, $n = 6$; $p < 0.05$; Fig. 1C).

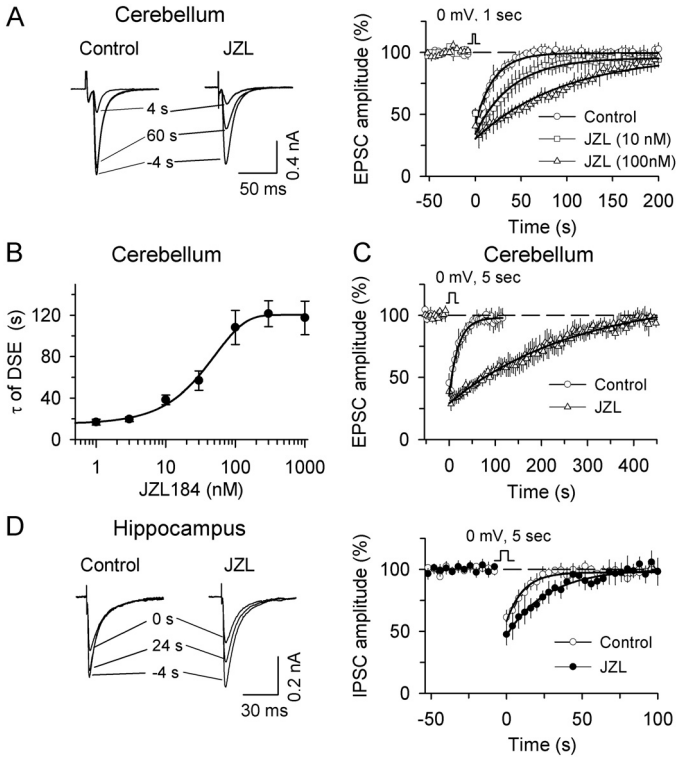

Fig. 1. MAGL inhibitor JZL184 (JZL) potentiates DSE mouse cerebellar Purkinje neurons and DSI in mouse hippocampal pyramidal neurons. A, Left, examples of EPSCs in Purkinje neurons 4 s before (−4 s), 4 s, and 60 s after the depolarization (1 s from −60 to 0 mV), in the presence of the solvent (DMSO, control) or JZL184. Right, time course of averaged DSE in slices treated with DMSO (control, $n = 8$) and different concentrations of JZL184 (JZL, 10 nM, $n = 8$; 100 nM, $n = 6$). The lines are single exponential fitting curves of the decay of DSE. B, JZL184 caused a dose-dependent increase in the decay time constant (τ) of DSE ($n = 4–8$ for each point). C, JZL184 (1 μM) dramatically prolonged DSE when longer depolarization (5 s from −60 to 0 mV) was used to induce DSE ($n = 6–8$). D, Left, examples of IPSCs in hippocampal pyramidal neurons 4 s before (−4 s), 0 s, and 24 s after the depolarization (5 s from −60 to 0 mV), in the presence of the solvent (DMSO) or JZL184. Right, time course of averaged DSI in slices treated with DMSO (control, $n = 10$) and 100 nM JZL184 ($n = 9$).

We next studied the effect of JZL184 on DSI in CA1 pyramidal neurons in mouse hippocampal slices. IPSCs were evoked every 4 s by stimulating inhibitory synaptic inputs, and a brief depolarization (5 s from −60 to 0 mV) was used to induce DSI (see *Materials and Methods*). Bath application of JZL184 (100 nM) significantly prolonged DSI (τ: control, 9.5 ± 2.9 s, $n = 10$; JZL184, 21.9 ± 2.6 s, $n = 9$; $p < 0.05$). The magnitude of DSI seemed to be increased by JZL184 (control, 31.8 ± 6.1%, $n = 10$; 100 nM JZL184, 45.6 ± 9.4%, $n = 9$); however, the difference between the control group and JZL184 group is not statistically significant ($p > 0.05$). Consistent with previous studies indicating that hippocampal DSI is mediated by CB1 receptor activation (Ohno-Shosaku et al., 2001; Wilson and Nicoll, 2001), it was found that the CB1 receptor antagonist AM 251 (2 μM) abolished DSI induced in the presence or absence of JZL184 ($n = 5$ each, data not shown).

JZL184 Selectively Amplifies the Effect of 2-AG, and URB597 Amplifies the Effect of AEA. Although JZL184 blocks MAGL activity with high selectivity and potency and does not affect FAAH activity in mouse brain membranes (Long et al., 2009a), its effectiveness and selectivity in brain slices have not been determined previously. Therefore, we examined the effects of both JZL184 and the selective FAAH inhibitor URB597 on the inhibitory effects of both exogenous AEA and 2-AG on EPSCs in mouse cerebellar slices. EPSCs were evoked every 10 s in these experiments. Bath application of 2-AG (10 μM) depressed EPSCs in Purkinje neurons (87.1 ± 6% of baseline, $n = 5$; $p < 0.05$), and this depression was significantly enhanced in the continuous presence of 100 nM JZL184 (67.6 ± 5.7% of baseline, $n = 5$; $p < 0.05$ versus 2-AG alone; Fig. 2A). Bath application of AEA (25 μM) induced similar depression of EPSCs in these neurons (85.7 ± 4.2% of baseline, $n = 4$; $p < 0.05$). However, JZL184 (100 nM) had no significant effect on AEA-induced depression of EPSCs (84.8 ± 4.7% of baseline, $n = 4$; $p > 0.05$ versus AEA alone; Fig. 2B).

Previous studies have shown that the selective FAAH inhibitor URB597 (Kathuria et al., 2003) amplifies the AEA-

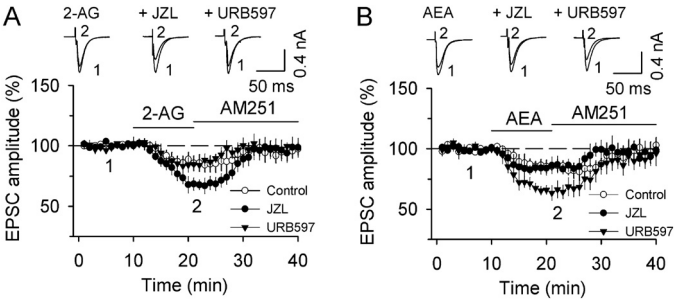

Fig. 2. MAGL inhibitor JZL184 selectively amplifies the effect of 2-AG, whereas FAAH inhibitor URB597 amplifies the effect of AEA. A, bath application of 2-AG (10 μM) depressed EPSCs in mouse cerebellar Purkinje neurons ($n = 5$). This depression was enhanced by JZL184 (JZL, 100 nM, $n = 5$), but not by URB597 (1 μM, $n = 3$). The 2-AG-induced depression of EPSCs was blocked by AM251 (2 μM). B, bath application of AEA (25 μM) depressed EPSCs in mouse cerebellar Purkinje neurons ($n = 4$). This depression was enhanced by URB597 (1 μM, $n = 3$), but not by JZL184 (JZL, 100 nM, $n = 4$). The AEA-induced depression of EPSCs was blocked by AM251 (2 μM).

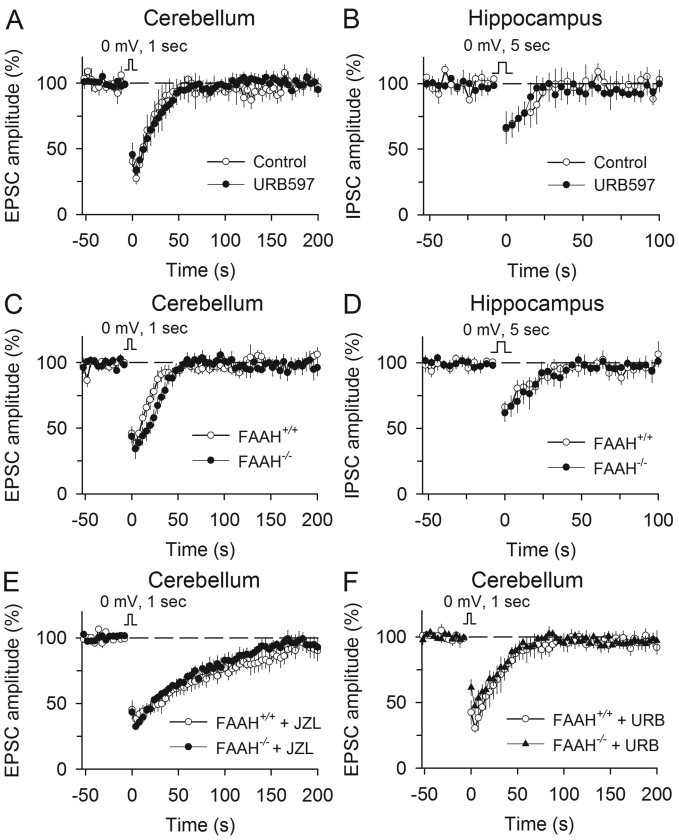

Fig. 3. Pharmacological blockade and genetic knockout of FAAH did not affect DSE and DSI. A, URB597 (1 μM) did not affect DSE in cerebellar Purkinje neurons ($n = 5$ each group). B, URB597 (1 μM) did not affect DSI in CA1 pyramidal neurons ($n = 9$–10). C and D, cerebellar DSE (C) and hippocampal DSI (D) were not significantly different in slices prepared from $FAAH^{-/-}$ and $FAAH^{+/+}$ mice ($n = 7$–9). E, JZL184 (JZL, 100 nM) prolonged DSE to a similar extent in cerebellar slices from $FAAH^{-/-}$ and $FAAH^{+/+}$ mice ($n = 7$ each group). F, URB597 did not affect DSE in slices from $FAAH^{-/-}$ and $FAAH^{+/+}$ mice ($n = 7$ each group).

induced depression of IPSCs in hippocampal neurons (Kim and Alger, 2004) and cerebellar Purkinje neurons (Szabo et al., 2006). Consistent with these findings, we found that URB597 (1 μM) significantly potentiated AEA-induced depression of EPSCs in mouse cerebellar Purkinje neurons (65.6 ± 5.4% of baseline, $n = 3$; $p < 0.05$ versus AEA alone; Fig. 2B). However, URB597 had no significant effect on 2-AG-induced depression of EPSCs (85.2 ± 5.2% of baseline, $n = 3$; $p > 0.05$ versus 2-AG alone; Fig. 2A). Both AEA- and 2-AG-induced depression of EPSCs were blocked by AM251 (2 μM), supporting the involvement of CB1 receptors. These data suggest that MAGL is the primary mechanism by which 2-AG is metabolized and that JZL184 is a selective MAGL inhibitor, whereas FAAH is the primary mechanism by which AEA is metabolized and URB597 is a selective FAAH inhibitor.

Effects of FAAH Inhibitor URB597 and FAAH Knockout on DSE and DSI. Previous studies have shown that URB597 has no significant effect on DSI in hippocampal and cerebellar slices (Kim and Alger, 2004; Makara et al., 2005; Szabo et al., 2006) and DSE in cultured autaptic hippocampal neurons (Straiker and Mackie, 2005). Consistent with these findings, we found that bath application of URB597 (1 μM) had no significant effect on either the magnitude or the decay time constant of DSE in mouse Purkinje neurons (τ: control, 17.6 ± 2.3 s, $n = 5$; URB597, 24.6 ± 6.7 s, $n = 5$; $p > 0.05$; Fig. 3A). Likewise, URB597 did not affect the magnitude or decay of DSI in mouse hippocampal pyramidal neurons (τ: control, 16.8 ± 2.6 s, $n = 9$; URB597, 13.8 ± 2.7 s, $n = 10$; $p > 0.05$; Fig. 3B).

FAAH knockout ($FAAH^{-/-}$) mice are severely impaired in their ability to degrade AEA (Cravatt et al., 2001). We examined the effect of FAAH knockout on DSE/DSI and found that the magnitude and decay time constant of DSE in cerebellar slices prepared from wild-type mice were not significantly different from the same parameters in $FAAH^{-/-}$ mice (τ: $FAAH^{+/+}$, 19.5 ± 3.8 s, $n = 7$; $FAAH^{-/-}$, 24.8 ± 1.8 s, $n = 7$; $p > 0.05$; Fig. 3C). Likewise, the magnitude and decay of DSI in hippocampal pyramidal neurons were also not different between $FAAH^{+/+}$ mice and $FAAH^{-/-}$ mice (τ: $FAAH^{+/+}$, 14.9 ± 3.6 s, $n = 9$; $FAAH^{-/-}$, 17.1 ± 3.8 s, $n = 8$; $p > 0.05$; Fig. 3D). Furthermore, preincubation of the cerebellar slices with JZL184 (100 nM) prolonged the decay time constant of DSE to a similar extent in $FAAH^{-/-}$ and $FAAH^{+/+}$ mice (τ: $FAAH^{+/+}$, 103.9 ± 18.6 s, $n = 7$; $FAAH^{-/-}$, 94.2 ± 14.9 s, $n = 7$; $p > 0.05$; Fig. 3E), whereas bath application of URB597 had no significant effect on DSE in these mice (τ: $FAAH^{-/-}$, 31.8 ± 4.2 s, $n = 7$; $FAAH^{+/+}$, 33.5 ± 5.8 s, $n = 7$; $p > 0.05$; Fig. 3F). FAAH is expressed by hippocampal pyramidal neurons and cerebellar Purkinje neurons (Tsou et al., 1998b; Cravatt et al., 2001; Gulyas et al., 2004). Because FAAH inhibitor URB597 was effective in enhancing AEA-induced depression of EPSCs in cerebellar Purkinje neurons (Fig. 2B), the lack of effect of URB597 and FAAH knockout on DSE and DSI suggests that AEA is not the eCB mediator for DSE and DSI.

JZL184 Potentiates DSE and DSI by Inhibiting MAGL. Although all currently available evidence indicates that JZL184 is a highly selective and potent MAGL inhibitor (Long et al., 2009a), it is possible that JZL184 potentiates DSE and DSI via mechanisms other than inhibition of MAGL. Two sets of experiments were performed to address this issue. In the first set of experiments, we examined the effects of JZL184 on DSE and DSI in rat neurons. ABPP of brain membranes has shown that JZL184 is ~10- to 100-fold less potent in inhibiting rat MAGL than in inhibiting mouse and human MAGL (Long et al., 2009b). If the inhibition of

MAGL accounts for the effect of JZL184 on DSE/DSI, we expect that potentiation of DSE/DSI in rat neurons is less than that in mouse neurons.

We first examined the effect of JZL184 on DSE in rat cerebellar Purkinje neurons. Bath application of a low concentration of JZL184 (100 nM) had no significant effect on the decay time constant of DSE (τ: control, 12.5 ± 1.5 s, n = 5; JZL184, 13.3 ± 1.9 s, n = 5; $p > 0.05$); however, at a higher concentration (1 μM), JZL184 significantly prolonged the decay time constant of DSE (τ: control, 11.4 ± 1.1 s, n = 7; 1 μM JZL184, 20.8 ± 2.1 s, n = 8; $p < 0.05$; Fig. 4A). Likewise, JZL184 at 1 μM significantly prolonged DSI in rat hippocampal pyramidal neurons (τ: control, 8.5 ± 1.2 s, n = 9; JZL184, 15.2 ± 1.7 s, n = 8; $p < 0.05$; Fig. 4B), but at 100 nM it had no significant effect on DSI (τ: control, 8.1 ± 1.3 s, n = 9; JZL184, 11.8 ± 1.9 s, n = 9; $p > 0.05$). We next examined the effect of selective FAAH inhibitor on DSE/DSI in rat neurons. We found that URB597 (1 μM) had no significant effect on DSE in rat Purkinje neurons (τ: control, 11.9 ± 1.4 s, n = 7; URB597, 13.6 ± 1.5 s, n = 6; $p > 0.05$; Fig. 4C) and DSI in rat hippocampal neurons (τ: control, 7.2 ± 0.8 s, n = 8; URB597, 8.9 ± 1.7 s, n = 8; $p > 0.05$; Fig. 4D), similar to its effects in mouse neurons.

In the second set of experiments, we examined the effect of MAFP, a nonselective inhibitor of both MAGL and FAAH (Goparaju et al., 1999), on DSE and DSI. Because FAAH inhibitor URB597 and FAAH knockout did not affect DSE and DSI (Fig. 3), the effect of MAFP on DSE and DSI cannot be attributed to its inhibition of FAAH. If JZL184 potentiates DSE/DSI by inhibiting MAGL, its effects should be mimicked by nonselective MAGL inhibitor MAFP. Previous studies have shown that MAFP prolongs DSI in hippocampal neurons (Hashimotodani et al., 2007; Makara et al., 2007), but its effect on DSE, to our knowledge, has not been examined. We found that bath application of MAFP (500 nM) prolonged the decay time constant of DSE in mouse Purkinje neurons (τ: control, 15.7 ± 1.9 s, n = 4; MAFP, 81.5 ± 12 s, n = 5; $p <$ 0.05; Fig. 5A) and rat Purkinje neurons (τ: control, 10.3 ± 1.4 s, n = 5; MAFP, 55.6 ± 9.2 s, n = 5; $p < 0.05$; Fig. 5B). Similarly, MAFP (500 nM) also significantly prolonged the decay time constant of DSI in CA1 pyramidal neurons in mouse hippocampal slices (τ: control, 15.9 ± 2.6 s, n = 10; MAFP, 28.9 ± 5.4 s, n = 8; $p < 0.05$; Fig. 5C) and rat hippocampal slices (τ: control, 8.8 ± 1.4 s, n = 9; MAFP, 24.3 ± 2.6 s, n = 10; $p < 0.05$; Fig. 5C). Unlike JZL184, the potentiation of DSE/DSI by MAFP in mouse neurons is comparable with that in rat neurons. Collectively, these experiments indicate that JZL184 exerts its effects on DSE and DSI by inhibiting MAGL.

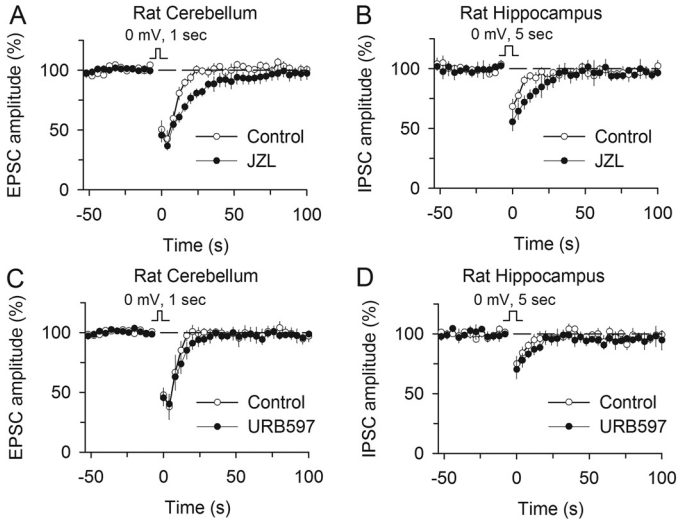

Fig. 4. Effects of MAGL inhibitor JZL184 (JZL) and FAAH inhibitor URB597 on DSE in rat neurons. A and B, JZL (1 μM) significantly prolonged DSE in rat cerebellar Purkinje neurons (A) and rat hippocampal pyramidal neurons (B). C and D, URB597 (1 μM) had no significant effect on DSE in rat cerebellar Purkinje neurons (C) and rat hippocampal pyramidal neurons (D).

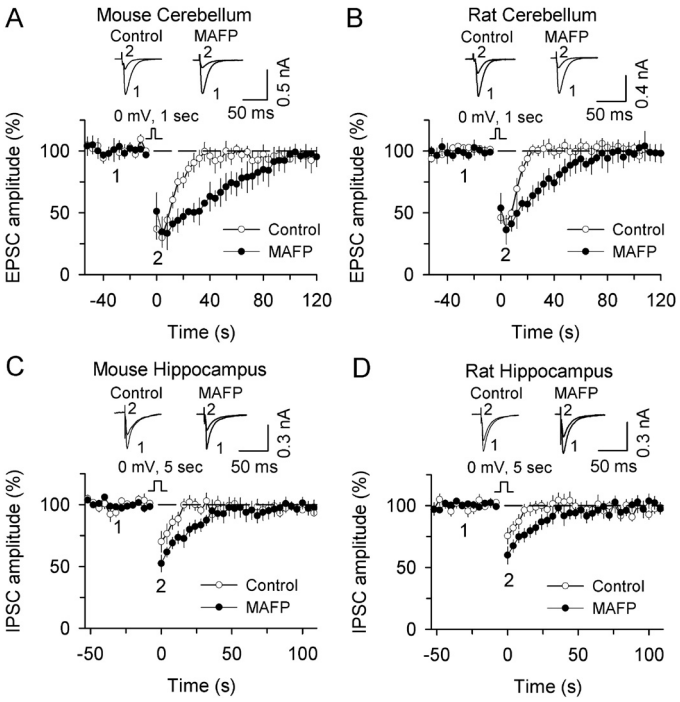

Fig. 5. The effect of nonselective MAGL inhibitor MAFP on DSE and DSI. A and B, MAFP (500 nM) prolonged DSE in mouse (A) and rat (B) cerebellar Purkinje neurons. C and D, MAFP (500 nM) prolonged DSI in mouse (C) and rat (D) hippocampal pyramidal neurons.

Discussion

In the present study, we find that DSE and DSI are potentiated by the MAGL inhibitors JZL184 and MAFP, but are not affected by the FAAH inhibitor URB597 or by genetic deletion of FAAH. MAGL is the primary enzyme that degrades 2-AG, whereas FAAH selectively degrades AEA (Cravatt et al., 1996; Blankman et al., 2007). The selective enhancement of DSE/DSI by JZL184 provides further evidence that 2-AG mediates DSE/DSI and that the degradation of 2-AG by MAGL determines the duration of DSE/DSI.

Many neurotransmitters achieve their diverse functions by activating multiple subtypes of receptors with a single ligand. However, the eCB system has at least two endogenous ligands, AEA and 2-AG, that activate the CB1 receptor (Di Marzo et al., 1998). Since the groundbreaking discoveries that DSE in the cerebellum and DSI in the hippocampus require CB1 receptor activation (Kreitzer and Regehr, 2001; Ohno-Shosaku et al., 2001; Wilson and Nicoll, 2001), there has been considerable interest in identifying the eCB mediator for DSE/DSI and understanding how the duration of DSE/DSI is regulated. Toward this end, the effects of block-

ing the degradative pathways of AEA and 2-AG on DSE/DSI have been examined. MAGL is the primary enzyme responsible for 2-AG hydrolysis, and approximately 85% 2-AG is hydrolyzed by MAGL (Blankman et al., 2007). On the other hand, the only hydrolytic enzyme in brain that uses AEA as a substrate is FAAH (Cravatt et al., 1996), as demonstrated by findings that pharmacological blockade or genetic knockout of FAAH dramatically increases AEA concentrations in the brain (Cravatt et al., 2001; Kathuria et al., 2003; Lichtman et al., 2004). The separation of the AEA and 2-AG degradative pathways allows selective potentiation of AEA- or 2-AG-dependent signaling by selective FAAH or MAGL inhibitors.

Previous studies have shown that blocking AEA degradation with selective FAAH inhibitor URB597 does not affect DSI in cerebellar Purkinje neurons (Szabo et al., 2006) and DSE/DSI hippocampal pyramidal neurons (Kim and Alger, 2004; Makara et al., 2005; Straiker and Mackie, 2005; Hashimotodani et al., 2007). We have found that URB597 and FAAH knockout do not affect DSE in cerebellar Purkinje neurons and DSI in hippocampal pyramidal neurons. These results add further evidence that AEA is not the eCB mediator for DSE/DSI, and FAAH does not regulate the time course of DSE/DSI. Several studies have shown that agents that inhibit both AEA and 2-AG catabolic pathways prolong the duration of DSI to variable degrees, although their effects on DSE have not been studied in brain slices. These agents include nonselective esterase and amidase inhibitors MAFP and arachidonoyl trifluoromethylketone (Szabo et al., 2006; Hashimotodani et al., 2007; Makara et al., 2007). As mentioned earlier, these inhibitors have multiple bioactive targets (Lio et al., 1996; De Petrocellis et al., 1997). Two previously identified MAGL inhibitors, URB754 and URB602 (Makara et al., 2005) also prolong DSI; however, recent studies have shown that neither URB754 nor URB602 affect 2-AG hydrolysis in rat brain (Saario et al., 2006), and the potentiation of DSI in rat hippocampal slices by URB754 is attributable to an impurity (Makara et al., 2007; Tarzia et al., 2007). In addition to catabolism by hydrolysis, both 2-AG and AEA are converted to the glycerol ester and ethanolamide of prostaglandins (Cravatt et al., 1996; Dinh et al., 2002). This occurs via the action of COX-2 and results in products that are not active at CB1 receptors (Hu et al., 2008; Long et al., 2009a). In support of a role for this pathway in the inactivation of eCB signaling, COX-2 inhibitors such as nimesulide and meloxicam have been shown to prolong DSI in hippocampal neurons (Kim and Alger, 2004; Hashimotodani et al., 2007).

The recently developed MAGL inhibitor JZL184 demonstrates a level of selectivity and potency that has not been seen in previous generations of MAGL inhibitors. First, competitive ABPP of brain membranes has shown that JZL184 displayed IC_{50} values of 6 to 8 nM and 4 μM for blockade of recombinant and mouse brain membrane MAGL and FAAH, respectively (Long et al., 2009a). Second, in vivo microdialysis has shown that JZL184 causes a robust increase in 2-AG levels without affecting AEA levels. When administered in vivo, JZL184 induced several CB1 receptor-dependent behavioral effects (Long et al., 2009a). Third, we show that JZL184 enhances 2-AG-induced depression of EPSCs in Purkinje neurons but has no significant effect on AEA-induced depression of EPSCs. Collectively, these data indicate that JZL184 is a highly selective and potent MAGL inhibitor. We have found that JZL184 produces robust potentiation of DSE in cerebellar Purkinje neurons and DSI in hippocampal pyramidal neurons. JZL184 produces greater potentiation of DSE/DSI in mouse brain slices than in rat brain slices, which is in accord with ABPP data showing that JZL184 is more potent in inhibiting mouse and human MAGL than in inhibiting rat MAGL (Long et al., 2009b). Thus, JZL184 exerts its effect on DSE/DSI by inhibiting MAGL.

Immunohistochemical and electron microscopic studies have shown that, in a number of brain regions, MAGL is located in presynaptic axon terminals, whereas FAAH is located in postsynaptic neurons (Gulyas et al., 2004). In the hippocampus, MAGL is present in axon terminals of granule cells, CA3 pyramidal cells and some interneurons, but not in the somata and dendrites of CA1 pyramidal neurons, whereas FAAH is present on the membrane of mitochondria and smooth endoplasmic reticulum in CA1 pyramidal neurons, but not in interneurons (Tsou et al., 1998b; Gulyas et al., 2004). In the cerebellum, MAGL is present in the axons in the molecular layer but absent in Purkinje cells, whereas FAAH is present in the somata and dendrites of Purkinje cells (Tsou et al., 1998b; Cravatt et al., 2001; Gulyas et al., 2004). CB1 receptors are exclusively distributed on presynaptic axonal terminals (Tsou et al., 1998a; Katona et al., 1999). The close proximity of the CB1 receptor and MAGL suggests that a primary function of MAGL is to limit the occupation of CB1 receptors by 2-AG. The findings that JZL184 and other MAGL inhibitors prolong DSE/DSI seem to support this notion.

MAGL is capable of hydrolyzing 2-AG and other monoacylglycerols such as monopalmitoylglycerol and monooleoylglycerol (Ho and Hillard, 2005; Long et al., 2009a). However, for reasons not fully understood, JZL184 selectively raises 2-AG levels but only minimally affects other monoacylglycerols (Long et al., 2009a). Moreover, these monoacylglycerols are not endogenous ligands that activate CB1 receptors. The potentiation of DSE/DSI by JZL184 suggests that degradation of 2-AG by MAGL is the rate-limiting step that determines the time course of retrograde eCB signaling in the brain. The present study also demonstrates that JZL184 is a useful tool to study 2-AG signaling.

References

Bisogno T, Ortar G, Petrosino S, Morera E, Palazzo E, Nalli M, Maione S, Di Marzo V, and Endocannabinoid Research Group (2009) Development of a potent inhibitor of 2-arachidonoylglycerol hydrolysis with antinociceptive activity in vivo. *Biochim Biophys Acta* **1791:**53–60.

Blankman JL, Simon GM, and Cravatt BF (2007) A comprehensive profile of brain enzymes that hydrolyze the endocannabinoid 2-arachidonoylglycerol. *Chem Biol* **14:**1347–1356.

Cravatt BF, Demarest K, Patricelli MP, Bracey MH, Giang DK, Martin BR, and Lichtman AH (2001) Supersensitivity to anandamide and enhanced endogenous cannabinoid signaling in mice lacking fatty acid amide hydrolase. *Proc Natl Acad Sci U S A* **98:**9371–9376.

Cravatt BF, Giang DK, Mayfield SP, Boger DL, Lerner RA, and Gilula NB (1996) Molecular characterization of an enzyme that degrades neuromodulatory fatty-acid amides. *Nature* **384:**83–87.

De Petrocellis L, Melck D, Ueda N, Maurelli S, Kurahashi Y, Yamamoto S, Marino G, and Di Marzo V (1997) Novel inhibitors of brain, neuronal, and basophilic anandamide amidohydrolase. *Biochem Biophys Res Commun* **231:**82–88.

Di Marzo V, Melck D, Bisogno T, and De Petrocellis L (1998) Endocannabinoids: endogenous cannabinoid receptor ligands with neuromodulatory action. *Trends Neurosci* **21:**521–528.

Dinh TP, Carpenter D, Leslie FM, Freund TF, Katona I, Sensi SL, Kathuria S, and Piomelli D (2002) Brain monoglyceride lipase participating in endocannabinoid inactivation. *Proc Natl Acad Sci U S A* **99:**10819–10824.

Goparaju SK, Ueda N, Taniguchi K, and Yamamoto S (1999) Enzymes of porcine brain hydrolyzing 2-arachidonoylglycerol, an endogenous ligand of cannabinoid receptors. *Biochem Pharmacol* **57:**417–423.

Gulyas AI, Cravatt BF, Bracey MH, Dinh TP, Piomelli D, Boscia F, and Freund TF (2004) Segregation of two endocannabinoid-hydrolyzing enzymes into pre- and postsynaptic compartments in the rat hippocampus, cerebellum and amygdala. *Eur J Neurosci* **20:**441–458.

Hashimotodani Y, Ohno-Shosaku T, and Kano M (2007) Presynaptic monoacylglycerol lipase activity determines basal endocannabinoid tone and terminates retrograde endocannabinoid signaling in the hippocampus. *J Neurosci* **27:**1211–1219.

Ho WS and Hillard CJ (2005) Modulators of endocannabinoid enzymic hydrolysis and membrane transport. *Handb Exp Pharmacol* :187–207.

Hu SS, Bradshaw HB, Chen JS, Tan B, and Walker JM (2008) Prostaglandin E2 glycerol ester, an endogenous COX-2 metabolite of 2-arachidonoylglycerol, induces hyperalgesia and modulates NFkappaB activity. *Br J Pharmacol* **153:**1538–1549.

Jung KM, Mangieri R, Stapleton C, Kim J, Fegley D, Wallace M, Mackie K, and Piomelli D (2005) Stimulation of endocannabinoid formation in brain slice cultures through activation of group I metabotropic glutamate receptors. *Mol Pharmacol* **68:**1196–1202.

Kathuria S, Gaetani S, Fegley D, Valiño F, Duranti A, Tontini A, Mor M, Tarzia G, La Rana G, Calignano A, et al. (2003) Modulation of anxiety through blockade of anandamide hydrolysis. *Nat Med* **9:**76–81.

Katona I, Sperlágh B, Sík A, Käfalvi A, Vizi ES, Mackie K, and Freund TF (1999) Presynaptically located CB1 cannabinoid receptors regulate GABA release from axon terminals of specific hippocampal interneurons. *J Neurosci* **19:**4544–4558.

Kim J and Alger BE (2004) Inhibition of cyclooxygenase-2 potentiates retrograde endocannabinoid effects in hippocampus. *Nat Neurosci* **7:**697–698.

King AR, Duranti A, Tontini A, Rivara S, Rosengarth A, Clapper JR, Astarita G, Geaga JA, Luecke H, Mor M, et al. (2007) URB602 inhibits monoacylglycerol lipase and selectively blocks 2-arachidonoylglycerol degradation in intact brain slices. *Chem Biol* **14:**1357–1365.

Kozak KR, Rowlinson SW, and Marnett LJ (2000) Oxygenation of the endocannabinoid, 2-arachidonylglycerol, to glyceryl prostaglandins by cyclooxygenase-2. *J Biol Chem* **275:**33744–33749.

Kreitzer AC and Regehr WG (2001) Retrograde inhibition of presynaptic calcium influx by endogenous cannabinoids at excitatory synapses onto Purkinje cells. *Neuron* **29:**717–727.

Lichtman AH, Leung D, Shelton CC, Saghatelian A, Hardouin C, Boger DL, and Cravatt BF (2004) Reversible inhibitors of fatty acid amide hydrolase that promote analgesia: evidence for an unprecedented combination of potency and selectivity. *J Pharmacol Exp Ther* **311:**441–448.

Lio YC, Reynolds LJ, Balsinde J, and Dennis EA (1996) Irreversible inhibition of Ca(2+)-independent phospholipase A2 by methyl arachidonyl fluorophosphonate. *Biochim Biophys Acta* **1302:**55–60.

Long JZ, Li W, Booker L, Burston JJ, Kinsey SG, Schlosburg JE, Pavón FJ, Serrano AM, Selley DE, Parsons LH, et al. (2009a) Selective blockade of 2-arachidonoylglycerol hydrolysis produces cannabinoid behavioral effects. *Nat Chem Biol* **5:**37–44.

Long JZ, Nomura DK, and Cravatt BF (2009b) Characterization of monoacylglycerol lipase inhibition reveals differences in central and peripheral endocannabinoid metabolism. *Chem Biol* **16:**744–753.

Maejima T, Hashimoto K, Yoshida T, Aiba A, and Kano M (2001) Presynaptic inhibition caused by retrograde signal from metabotropic glutamate to cannabinoid receptors. *Neuron* **31:**463–475.

Makara JK, Mor M, Fegley D, Szabó SI, Kathuria S, Astarita G, Duranti A, Tontini A, Tarzia G, Rivara S, et al. (2005) Selective inhibition of 2-AG hydrolysis enhances endocannabinoid signaling in hippocampus. *Nat Neurosci* **8:**1139–1141.

Makara JK, Mor M, Fegley D, Szabo SI, Kathuria S, Astarita G, Duranti A, Tontini A, Tarzia G, Rivara S, et al. (2007) Corrigendum: Selective inhibition of 2-AG hydrolysis enhances endocannabinoid signaling in hippocampus. *Nat Neurosci* **10:**134.

Ohno-Shosaku T, Maejima T, and Kano M (2001) Endogenous cannabinoids mediate retrograde signals from depolarized postsynaptic neurons to presynaptic terminals. *Neuron* **29:**729–738.

Pitler TA and Alger BE (1992) Postsynaptic spike firing reduces synaptic GABAA responses in hippocampal pyramidal cells. *J Neurosci* **12:**4122–4132.

Saario SM, Palomäki V, Lehtonen M, Nevalainen T, Järvinen T, and Laitinen JT (2006) URB754 has no effect on the hydrolysis or signaling capacity of 2-AG in the rat brain. *Chem Biol* **13:**811–814.

Saario SM, Salo OM, Nevalainen T, Poso A, Laitinen JT, Järvinen T, and Niemi R (2005) Characterization of the sulfhydryl-sensitive site in the enzyme responsible for hydrolysis of 2-arachidonoyl-glycerol in rat cerebellar membranes. *Chem Biol* **12:**649–656.

Simon GM and Cravatt BF (2008) Anandamide biosynthesis catalyzed by the phosphodiesterase GDE1 and detection of glycerophospho-N-acyl ethanolamine precursors in mouse brain. *J Biol Chem* **283:**9341–9349.

Stella N, Schweitzer P, and Piomelli D(1997) A second endogenous cannabinoid that modulates long-term potentiation. *Nature* **388:**773–778.

Straiker A and Mackie K (2005) Depolarization-induced suppression of excitation in murine autaptic hippocampal neurones. *J Physiol* **569:**501–517.

Szabo B, Urbanski MJ, Bisogno T, Di Marzo V, Mendiguren A, Baer WU, and Freiman I (2006) Depolarization-induced retrograde synaptic inhibition in the mouse cerebellar cortex is mediated by 2-arachidonoylglycerol. *J Physiol* **577:**263–280.

Tarzia G, Antonietti F, Duranti A, Tontini A, Mor M, Rivara S, Traldi P, Astarita G, King A, Clapper JR, et al. (2007) Identification of a bioactive impurity in a commercial sample of 6-methyl-2-p-tolylaminobenzo[d][1,3]oxazin-4-one (URB754). *Ann Chim* **97:**887–894.

Tsou K, Brown S, Sañudo-Peña MC, Mackie K, and Walker JM (1998a) Immunohistochemical distribution of cannabinoid CB1 receptors in the rat central nervous system. *Neuroscience* **83:**393–411.

Tsou K, Nogueron MI, Muthian S, Sañudo-Pena MC, Hillard CJ, Deutsch DG, and Walker JM (1998b) Fatty acid amide hydrolase is located preferentially in large neurons in the rat central nervous system as revealed by immunohistochemistry. *Neurosci Lett* **254:**137–140.

Vandevoorde S, Jonsson KO, Labar G, Persson E, Lambert DM, and Fowler CJ (2007) Lack of selectivity of URB602 for 2-oleoylglycerol compared to anandamide hydrolysis in vitro. *Br J Pharmacol* **150:**186–191.

Wilson RI and Nicoll RA (2001) Endogenous cannabinoids mediate retrograde signalling at hippocampal synapses. *Nature* **410:**588–592.

Address correspondence to: Dr. Qing-song Liu, Department of Pharmacology and Toxicology, Medical College of Wisconsin, 8701 Watertown Plank Road, Milwaukee, WI 53226. E-mail: qsliu@mcw.edu